COLOUR CONSTANCY FOR NON-UNIFORM ILLUMINANT USING IMAGE TEXTURE

M. A. Hussain *, A. Sheikh Akbari† and B. Mallik†

**†School of Computing, Creative Technology and Engineering, Faculty of Arts, Environment and Technology, Leeds Beckett University, U.K., *m.hussein7766@student.leedsbeckett.ac.uk*

Keywords: colour constancy, non-uniform illuminant, image segmentation, texture.

Abstract

Colour constancy (CC) is the ability to perceive the true colour of the scene on its image regardless of the scene's illuminant changes. Colour constancy is a significant part of the digital image processing pipeline, more precisely, where true colour of the object is needed. Most existing CC algorithms assume a uniform illuminant across the whole scene of the image, which is not always the case. Hence, their performance is influenced by the presence of multiple light sources. This paper presents a colour constancy algorithm using image texture for uniform/non-uniformly lit scene images. The propose algorithm applies the K-means algorithm to segment the input image based on its different colour feature. Each segment's texture is then extracted using the Entropy analysis algorithm. The colour information of the texture pixels is then used to calculate initial colour constancy adjustment factor for each segment. Finally, the colour constancy adjustment factors for each pixel within the image is determined by fusing the colour constancy of all segment regulated by the Euclidian distance of each pixel from the centre of the segments. Experimental results on both single and multiple illuminant image datasets show that the proposed algorithm outperforms the existing state of the art colour constancy algorithms, particularly when the images lit by multiple light sources.

1 Introduction

The view of an image scene, captured by a digital imaging device, depends on the frequency of the reflected light corresponding to the colour of the object, the sensitivity functions of the device and the presence of illuminant on the scene [1]. Therefore, the appearance of a digital image is influenced by the spectrum of the illuminant, which may create undesired colour cast within the image [2]. For instance, the image of a white object captured under a very bright illuminant will have bluish colour cast and it could have a red or yellow colour cast under low lighting condition [3]. Human visual system can perceive the original colour of an object by adjusting the spectral response and distinguishing the colour of the source illuminant, while digital imaging devices such as cameras and mobile phones, in most cases fail to adapt to the illuminant spectral changes efficiently [4,5]. The aim of the colour constancy algorithms is to adjust the colour of a colour casted image so that it appears as if it has been taken under canonical light [6,7]. Researchers have proposed varicose techniques to perform colour constancies. Grey World [8] is one of the colour constancy adjustment methods, which is considered as a best performer for the images having sufficient colour variation [9]. The Grey World [8] algorithm's assumption is based on the principle that the average reflectance of each colour component of a scene illuminated by a natural light source is representative of the grey level. The performance of the Grey world algorithm is deteriorated in presence of a large uniform colour patch in the scene [10]. Max-RGB, also known as White Patch method, assumes that the maximum values of the RGB-channels represent a pure white colour. Hence, it uses the maximum of the image RGB-channels information to adjust colour constancy of the image [11]. Since the human eyes are more sensitive to the luminosity of green channel, Lam [12] improved the Max-RGB method's performance by leaving the green channel colour unchanged and adjust the red and blue components of the image using the Max-RGB technique. Nevertheless, the dependency of these techniques on the brightest pixel of the image often lead to erroneous results particularly for images with lower intensity [13]. Finlayson et al. [14] proposed a method to overcome the data dependency of the Grey World and the Max-RGB methods by incorporating Minkowski Norm p, which means assigning higher weights to the pixels with higher values. This algorithm sometime over saturates the images. Van de Weijer et al. [15] have shown that the image edges contain important image intensity information. Hence, they used image edge information to estimate the image illuminant. The Weighted Grey Edge method, which is an extension of the Grey Edge method, was reported by Gisenji et al. [16]. This method incorporates general weighting scheme of the Grey Edge method and the edge of the shadows within the image to perform colour constancy adjustment. Most of the existing colour constancy algorithms assume that the scene is illuminated by a single light source. However, this assumption is considered to be inappropriate in real life scenarios as a scene usually is lit by multiple illuminants [17,18].

This paper presents a colour constancy algorithm for single and multiple illuminant using the texture of image segments. The proposed algorithm applies the K-mean algorithm to split the input image into a number of segments. It then performs entropy analysis on each resulting segment's pixels to extract the texture information of the segment. The Grey World Theorem is then used to calculate initial colour constancy factors for the segment using pixels identified by texture map of the segment. Finally, colour constancy adjustment factor for each pixel is determined by fusing the colour constancy adjustment factors of all segments regulated by the Euclidian distance of the pixel from the centre of each segment. Experimental results on two image datasets demonstrate that the proposed techniques images exhibit significantly higher colour constancy to that of state of art techniques. The rest of the paper is organised as follows: Section 2 describes the proposed algorithm, Section 3 contains discussion on experimental result and Section 4 concludes the paper.

2 Proposed colour constancy adjustment method

The proposed colour constancy adjustment for multiple illuminant images by fusing the colour constancy information of the image segments includes three sections: image segmentation using the K-means algorithm, texture extraction and segment's colour constancy weighting factors calculation, and fusing segments' colour constancy factors.

2.1 Image segmentation using the K-means algorithm

Figure 1 shows the block diagram of the image segmentation using k-means clustering algorithm. An RGB image, the number of clusters that image needs to be split to and the number of iterations, shown as: *noi* in the block diagram, are input to the algorithm. To ease the segmentation process using the colour differences, the input image is first converted to the L*a*b* colour space, where a* and b* components contain the colour information of the image. The K-means clustering algorithm is used to divide the input image pixels into a number of segments based on their colour properties. The centroid selection and segmentation steps of the K-means algorithm are as follows:

i. Randomly select the initial n centroids of the segments from a* and b* components of the input image which are named as $(c_1 \dots c_n)_{i=0}$ and assign zero to i, where i represents the current iteration.
ii. Segment a* and b* components' coefficients into n segments based on their minimum Euclidian distances to the current n centroids, generating n segments named: $(cl_1 \dots cl_n)_i$.
iii. Determine the n new centroids, named $(c_1 \dots c_n)_i$ in Fig. 1, by calculating the average of the coefficients in each resulting segment and increment i variable by one.
iv. Check if i is greater than the predefined number of iteration (*noi*), if i is greater than *noi*, the previously determined segments, $(cl_1 \dots cl_n)_i$, are the final segments. Re-name them as: $cl_1 \dots cl_n$, as shown in the block diagram and the segmenting process is completed; otherwise go back to step ii.

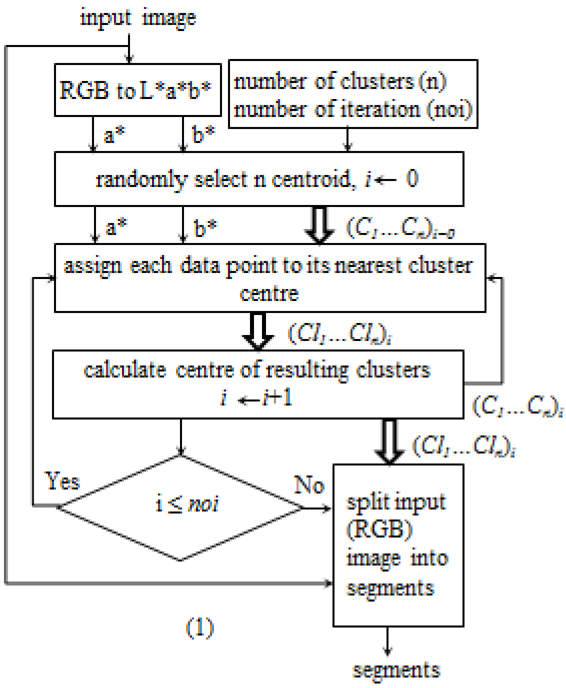

Figure 1: Block diagram of the k-means image segmentation algorithm.

2.2 Texture extraction and segment's colour constancy weighting factors calculation

Figure 2 shows the block diagram of the proposed texture extraction, segment selection and segment initial colour constancy weighting factors calculation method. Each resulting segment from Section 2.1 is processed independently as follows:

i. Convert segments pixels to grey.
ii. Calculate an entropy value for each pixel of the segment (entropy value is the statistical measure of the randomness that is used to characterised the texture of the input segment) using a 9×9 neighbouring values [19].
iii. Convert each segment's pixel's entropy value to an 8-bit grey value.
iv. Convert resulting grey segment pixels to a binary segment using two empirical threshold values.
v. If the resulting binary segment containing non-zero pixels, calculates center of non-zero pixels and set the segment's relevant bit in the decision vector (DV) (The DV was initialised to zero).
vi. Determine segment's initial colour constancy weighting factors using RGB image pixel values identified by binary segment pixels, the weighting factors for red, green and blue components are named K_{Ri}, K_{Gi} and K_{Bi} in the block diagram, respectively. The Grey World theorem is used to calculate the weighting factors, as shown in equation (2):

$$K_{IC} = {T_{mean}}\Big/{\frac{\sum T_C}{N}} \quad (2)$$

Where K_{IC} is the initial weighting factor for component C and $C \in \{R, G, B\}$, T_{mean} is the average value of the image pixels, identified by the non-zero binary segment's pixels, $\sum P_C$ is the sum of the identified pixels' component C values and N is the total number of identified pixels.

2.3 Fusing segments' initial colour constancy weighting factors

Figure 3 shows the block diagram of the proposed colour constancy weighting factors (CCWF) calculation for each pixel by fusing initial CCWF of the selected segments. From this figure, can be seen that the algorithm takes the selected segments' centers, C1, C2, …, Cn, RGB input image, decision vector (DV) and initial colour constancy weighting factors of all selected segments and calculate the weighting factors for each pixel's colour components, as shown in the following steps:

i. Calculate Euclidian distance of the pixel from the centers of all selected segments, named: ΔE_1, ΔE_2, … ΔE_n in the block diagram, using equation (3):

$$\Delta \mathrm{E_i} = \sqrt{(\mathrm{C_{ri}} - P_r)^2 + (\mathrm{C_{ci}} - P_c)^2} \quad (3)$$

where C_{ri} and C_{ci} represent row and column of the segment i center, respectively. Pr and Pc are the rows and columns position of the pixel, respectively and ΔE_i is the Euclidian distance of the pixel from the center of the segment i.

ii. The colour constancy adjustment factors, K_R , K_G and K_B for red, green and blue colour component of the pixel, respectively, are calculated by fusing the initial colour constancy weighting factors of the selected segments using equation (4):

$$k_C = \frac{\Delta E_1}{\Delta E_1 + \Delta E_2 + \cdots + \Delta E_n}(k_{C1}) + \frac{\Delta E_2}{\Delta E_1 + \Delta E_2 + \cdots + \Delta E_n}(k_{C2}) + \cdots + \frac{\Delta u_n}{\Delta E_1 + \Delta E_2 + \cdots + \Delta E_n}(k_{Cn}) \quad (4)$$

where k_C is the weighing factor for component C of the pixel, $C \in \{R, G, B\}$, ΔE_i is the Euclidian distance of the pixel from the center of the segment i, k_{C1} k_{C2}, and k_{Cn} are the initial colour constancy weighting factor for colour component C of the segment 1, 2, and n, respectively.

iii. Scale the R, G and B colour components of the input pixel by the resulting colour constancy weighting factors of stage ii.

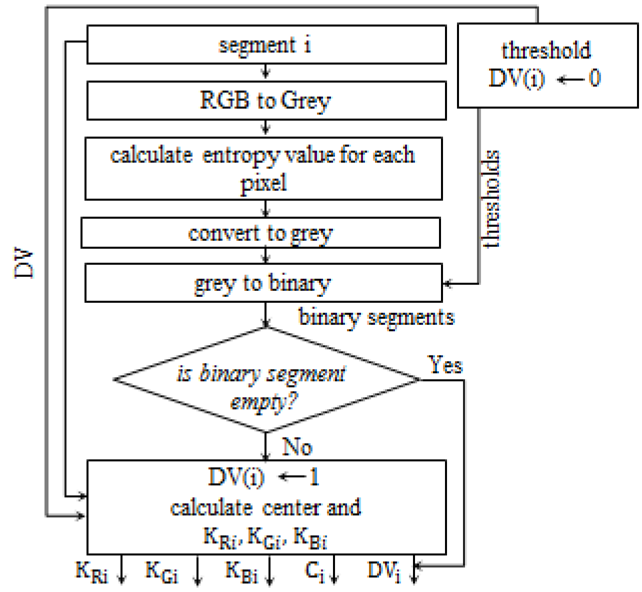

(2)

Figure 2: Block diagram of the proposed texture extraction, segment selection and segment initial colour constancy weighting factors calculation method.

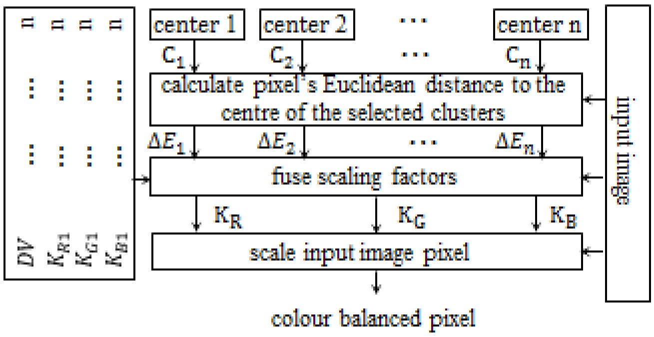

(3)

Figure 3: Block diagram of the proposed colour constancy weighting factors (CCWF) calculation for each pixel by fusing initial CCWF of the selected segments.

3 Experimental results

To evaluate the performance of the proposed method, the proposed method, Grey World [8], Max-RGB [11], Shades of Grey [14], 1st Order Grey Edge [15], 2nd Order Grey Edge [15] and Weighted Grey Edge [16] state of the arts colour constancy techniques was applied to the images of the three benchmark image datasets, called: Grey Ball dataset [20], MIRF dataset [21] and Multiple Light Source dataset [22]. The datasets are introduced sub-section 3.1 and evaluation is given in sub-section 3.2:

3.1 Dataset

Single illuminant dataset:

1. The Grey Ball dataset were captured by Ciuera and Funt [20] contains 11,340 images of size 240×360, mounting a grey ball in front of the imaging device. The surface area of the grey ball then used to evaluate the scene illuminant.

Multiple illuminant dataset:

2. MIRF dataset prepared by Beigpour et al. [21]. It consists of a laboratory part, for images taken in a closed room under controlled settings, and a real-world part, for images taken in various other environments.

3. Multiple Light Sources dataset was prepared by Gisenji et al. [22]. It includes several indoor and outdoor scenes under various lighting conditions. For indoor images, two halogen lights with the same specification were used. Four colour filters were used to obtain different colours of the light source.

3.2 Evaluation

The proposed method, Grey World, Max-RGB, Shades of Grey, 1st Order Grey Edge, 2nd Order Grey Edge and Weighted Grey Edge colour constancy algorithms were applied to the images of the above-named image datasets. The resulting images were subjectively evaluated. Results shows that the proposed technique's images exhibit the highest colour constancy, particularly for the images lit by multiple illuminant and for the images with large uniform colour patch.

To give an insight into the algorithm, an image from the Grey Ball dataset is taken and the proposed algorithm was applied on the image to divide the image into four segments. Figure 4 shows the original image and its resulting segments. The extracted texture for the segment 4 of the image, which mainly covers the uniform are of the image (sky), using the entropy analysis algorithm is shown in Figure 5. To select the pixels of a segment, which have sufficient information to be used for colour constancy adjustment, an investigation on indoor and outdoor images of the three above mentioned image datasets was carried out. It was empirically found that threshold range [0.3, 0.7] of the normalised texture values of the segment is a good measure to select the pixels. Further investigation on the number of segments needed for the proposed algorithm to efficiently operate were also carried out. It was found that selection of 4 segments and the number of iteration (*noi*) 5 are sufficient for the proposed algorithm to significantly outperform the state of art techniques without adding too much computational complexity.

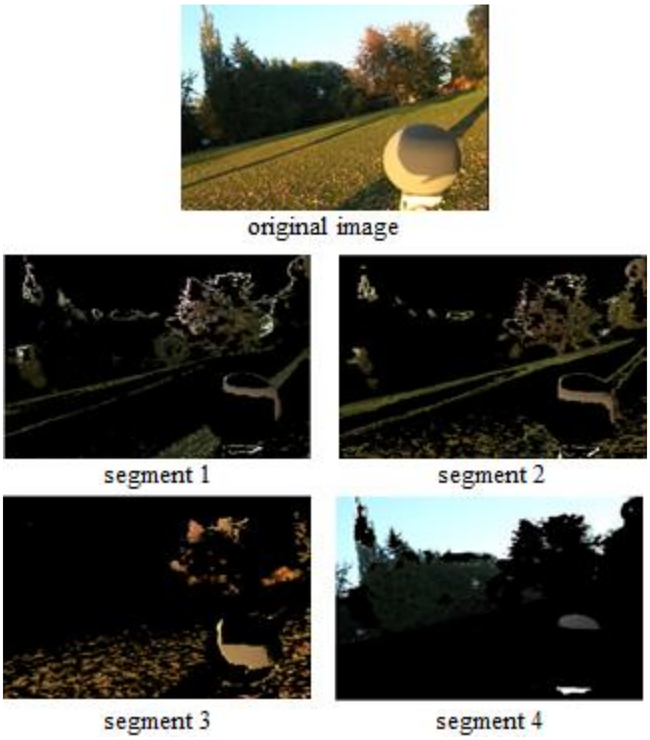

Figure 4: Original and its four resulting segments using the proposed algorithm.

Figure 5: Segment 4 of the image shown in Figure 4 and it's resulting texture analysis.

To give a sense of the achieved colour constancy and to enable the viewer to compare the achieved results, two images from the Grey Ball and Multiple Light Sources datasets with different visual contents, including uniform colour patches and multiple illuminant, were chosen and colour balanced using the proposed and the state of the art techniques. The resulting images are shown Figure 5-6, respectively. Figure 6a shows the input image taken from the grey ball dataset. Figure 6b, shows the Grey World image. From this image the existence of the colour cast on the tree branches is obvious. Figure 6c shows the Max-RGB image. This figure does not show any noticeable improvement either in the foreground or background objects of image. Figure 6d illustrates the Shades of Grey's image. This image shows some reduction of colour saturation significantly. However, the tree branch and shore area of the image still exhibits yellow colour cast. Figure 2e shows the 1st Order Grey Edge method's image. This image demonstrates less colour cast compare to that of the Grey World method's image. However, the grey ball area of the image still suffers from some level of the yellow colour cast. The 2nd Order Grey Edge method's image, shown in Figure 6f, shows higher colour constancy compared to the previously mentioned methods' images. The grey ball area of the image appears to have reduced level of yellow tint. Nonetheless, the shore and the tree branch area of the image still have some

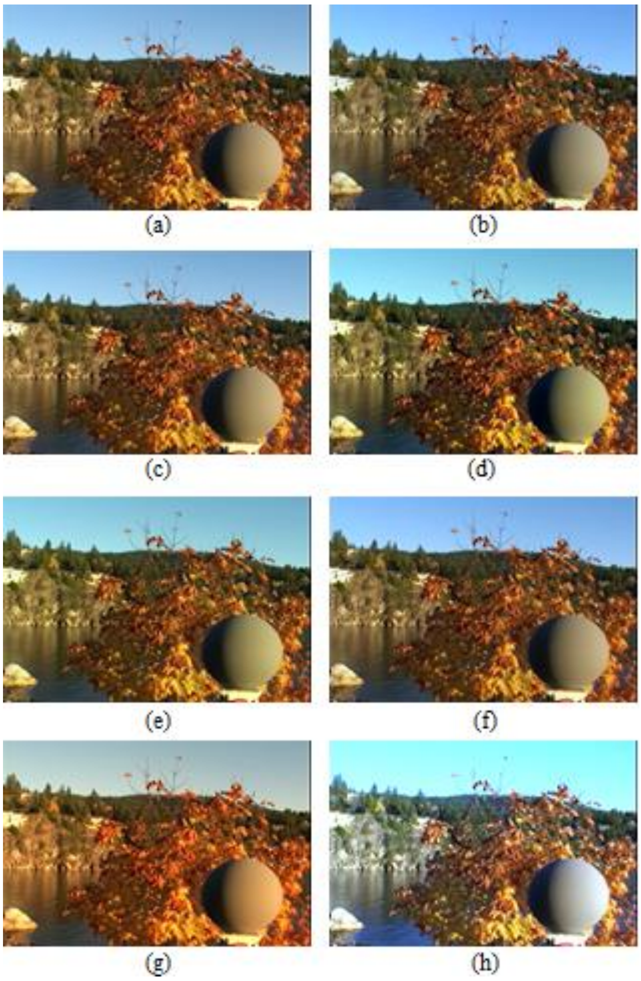

Figure 6: Original and colour balanced images from different techniques: a) Original image, b) Grey World, c) Max-RGB, d) Shades of Grey, e) 1st Order Grey Edge, f) 2nd Order Grey Edge, g) Weighted Grey Edge and h) Proposed method's images.

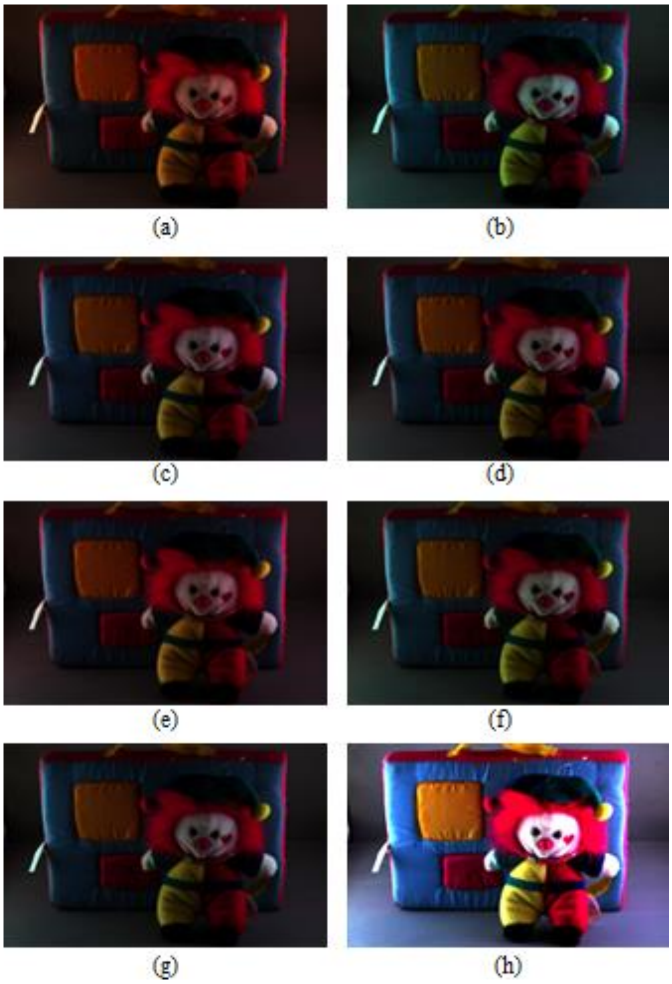

Figure 7: Original and colour balanced images from different techniques: a) Original image, b) Grey World, c) Max-RGB, d) Shades of Grey, e) 1st Order Grey Edge, f) 2nd Order Grey Edge, g) Weighted Grey Edge and h) Proposed method's images.

colour cast. An extreme presence of yellow saturation demonstrates by the Weighted Grey Edge method's image, illustrated in Figure 6g. The grey ball, tree branch and the shore areas of the image are erroneously showered by the source illuminant. The proposed method's image is shown in Figure 6h. This image manifests a natural 'true grey' colour ball and there is no sign of any colour casts on tree branch and the shore area of the image. The image appears as if it has been taken under canonical light.

Figure 7a shows the second original input image. This image has a darker background and the colour of the objects within the image is saturated to red and orange. Figure 7b shows the Grey World methods' image. This image exhibits lower red-orange colour cast. However, it has turned the colour cast of the image to green. Figure 7c illustrates the Max-RGB method's image. This image exhibits much natural lighting from an artificial hue. However, the actual colour of the image objects is not clearly visible in this image. The Shades of Grey's image is presented in Figure 7d. This image contains much lower colour casting and the doll and the bag area of the image appear comparatively natural. However, the floor and the background colour of the image demonstrate no noticeable colour constancy improvement. The 1st Order Grey Edge method's image is shown in Figure 7e. This image demonstrates a minor improvement on colour cast reduction but not sufficient improvement to exhibits the true colour of the doll, bag and the floor. Figure 7f demonstrates the 2nd Order Grey Edge technique's image. Figure 7g presents the Weighted Grey Edge methods' image. The performance of this algorithm is much higher than the previously discussed images. However, this image looks darker in whole, which make it difficult to observe the true colour of the image. The colour cast of the image somehow is being hidden behind the darkness of the image. The proposed methods' image is shown in Figure 7h. This image looks as if it has been taken under canonical light, despite the scene was illuminated by multiple light sources. No colour casts can be seen in the bag, doll and the floor of the image and the image looks so natural. In compare to other state of the art images, the proposed technique's image has the highest colour constancy.

4 Conclusions

In this paper, a colour constancy algorithm for single and multiple illuminant using the texture of the image segments was presented. The K-means algorithm was used to split the image into its colour segments. The texture of each image was generated using the entropy analysis. The resulting segments' texture information was used to select the pixels with sufficient colour information to be used for colour adjustment. The initial colour constancy weighting factors for each segment was determined using the selected pixels and the Grey World theorem. Colour constancy weighting factor for each pixel finally determined by fusing the calculated initial colour constancy weighting factor of all segments weighted regulated by the Euclidian distance of the pixel from the centroids of different segments. Experimental results using benchmark single and multiple illuminant image datasets approved that the proposed algorithm outperforms the state of the art methods.

References

[1] N. Banić, S. Lončarić. "Color Cat: Remembering Colors for Illumination Estimation", *IEEE Signal Processing Letters*, **22**(6), pp. 651-655, (2015).

[2] G. Schaefer, S. Hordley, G. Finlayson. "A combined physical and statistical approach to colour constancy", *IEEE Computer Society Conference on Computer Vision and Pattern Recognition*,**1,** pp. 148-153, (2005).

[3] T. Jiang, D. Nguyen, K. Kuhnert. "Auto White Balance Using the Coincidence of Chromaticity Histograms", *Eighth International Conference on Signal Image Technology and Internet Based Systems*, pp.201-208, (2012).

[4] A. Gijsenij, T. Gevers. "Color Constancy by Local Averaging", *14th International Conference on Image Analysis and Processing Workshops*, pp.171-174, (2007).

[5] S. B. Gao, K. F. Yang, C. Y. Li, Y. J. Li. "Color Constancy Using Double-Opponency", *IEEE Transactions on Pattern Analysis and Machine Intelligence*, **37** (10), pp. 1973-1985, (2015).

[6] H. R. V. Joze, M. S. Drew. "Exemplar-Based Color Constancy and Multiple Illumination", *IEEE Transactions on Pattern Analysis and Machine Intelligence*, **36**(5), pp. 860-873, (2014).

[7] S. J. J. Teng. "Robust Algorithm for Computational Color Constancy", *International Conference on Technologies and Applications of Artificial Intelligence*, pp. 1-8, (2010).

[8] G. Buchsbaum. "A spatial processor model for object colour perception", *Journal of the Franklin Institute*, vol. **310**(1), pp. 1–26, (1980).

[9] S. Tai, T. Liao, Y. Chang, C. Yeh. "Automatic White Balance algorithm through the average equalization and threshold", *8th International Conference on Information Science and Digital Content Technology*, pp. 571-576, (2012).

[10] A. Gijsenij, T. Gevers, J. Van de Weijer. "Computational Color Constancy: Survey and Experiments", *Image Processing, IEEE Transactions*, **20**(9), pp.2475-2489, (2011).

[11] E. Land. "The retinex theory of colour vision", *Scientific American*, **237**(6), pp. 108–128, (1977).

[12] E.Y. Lam. "Combining grey world and Retinex theory for automatic white balance in digital photography", *Proceedings of the International Symposium on Consumer Electronics*, pp. 134–139, (2005).

[13] N. Banić, S. Lončarić. "Improving the white patch method by subsampling," *IEEE International Conference on Image Processing*, pp. 605-609, (2014).

[14] G.D. Finlayson, E. Trezzi. "Shades of grey and colour constancy", *Proc. IS&T/SID Color Imaging Conf.*, pp. 37-41, (2004).

[15] J. van de Weijer, T. Gevers, A. Gijsenij. "Edge based colour constancy", *IEEE Trans on Image Processing*, pp.2 207-2217, (2007).

[16] A. Gijsenij, T. Gevers, J. Van de Weijer. "Improving Color Constancy by Photometric Edge Weighting," *IEEE Trans. on Pattern Analysis and Machine Intelligence*, **34**(5), pp. 918-929, (2012).

[17] M. Bleier *et al.*, "Color constancy and non-uniform illumination: Can existing algorithms work?", *IEEE International Conference on Computer Vision Workshops*, pp. 774-781, (2011).

[18] C. Riess, E. Eibenberger, E. Angelopoulou. "Illuminant color estimation for real-world mixed-illuminant scenes", IEEE *International Conference on Computer Vision Workshops)*, pp.782-789, (2011).

[19] Gonzalez, R.C., Woods, R.E., and Eddins, S.L.: "*Digital Image Processing Using MATLAB"*, Chapter 11, New Jersey, Prentice Hall, 2003.

[20] F. Ciurea, B. Funt. "A Large Image Database for Color Constancy Research", *Proceedings of the Imaging Science and Technology Eleventh Color Imaging Conference*, pp. 160-164, (2003).

[21] S. Beigpour, C. Riess, J. van de Weijer, E. Angelopoulou. "Multi-Illuminant Estimation with Conditional Random Fields", *IEEE Transactions on Image Processing*, **23**(1), pp. 83-96, (2014).

[22] A. Gijsenij, R. Lu, T. Gevers. "Color Constancy for Multiple Light Sources", *IEEE Transactions on Image Processing*, **21**(2), pp. 697-707, (2012).